JOURNAL OF MATERIALS SCIENCE 12 (1977) 1477–1483

Hydrostatic extrusion of solid polymers

Part 6 *Plastic deformation of high density polyethylene during hydrostatic extrusion*

KAZUO NAKAYAMA, HISAAKI KANETSUNA
Research Institute for Polymers and Textiles, Sawatari 4, Kanagawa-ku, Yokohama 221, Japan

Hydrostatic extrusion of a high density polyethylene rod was carried out. Both the process of plastic deformation during hydrostatic extrusion and the changes of properties of the polyethylene with extrusion were studied. Particular attention was paid to the process of molecular orientation and the destruction of the original lamellae. To obtain a better understanding of the deformation process, the lateral dimension of crystallite and the long period were obtained from the X-ray diffraction data. Furthermore, the influence of extrusion conditions on the structure and properties of the extrudate were investigated. The Vickers hardness number and thermal shrinkage of the extrudates were affected considerably by the extrusion conditions, i.e. extrusion temperature and extrusion ratio. In order to determine the relationship between the properties and extrusion conditions, it is necessary to consider not only the molecular orientation but also the crystallinity, fibrosity and the fine-structure of the extrudates.

1. Introduction

The structural changes of crystalline polymers accompanied by different modes of deformation have been investigated by many authors [1–4]. Drawing of a crystalline polymer represents changes in orientation of the molecular chains [5] and the transformation of the microspherulitic structure into an anisotropic fibre structure [6]. In general, molecular orientation can change the mechanical properties of polymers, and therefore the effects of plastic deformation are of great importance in the discussion of the physical properties of solid polymers.

In the first three papers of this series [7–9], the effects of extruding conditions on the deformation of high density polyethylene rods were investigated. In Parts 4 and 5 we discussed the molecular orientation and structural changes of polyacetal resin [10] and polyethylene [11] due to hydrostatic extrusion. It was apparent that hydrostatic extrusion and stretching had much in common with the orientation and deformation behaviour of polyethylene.

A detailed study of the wide- and small-angle X-ray diagrams in the necking portions of the cold-drawn polyethylene was made by Kasai and Kakudo [12]. Baltá-Calleja and Peterlin [13] made small-angle X-ray scattering investigations on the plastic deformation of a narrow film strip of polyethylene. In the experiments on the direct extrusion of polyethylene by Imada *et al.* [4], X-ray diffraction patterns of the longitudinal section of the extrudate were obtained to study the process of the development of crystal orientation in the die hole. It is of particular interest to study the process of plastic deformation along the flow line of hydrostatically extruded polyethylene.

This paper deals in the main part with effects of extrusion temperature and extrusion ratio on the plastic deformation of high density polyethylene. Particular attention has been paid to the process of molecular orientation and the destruction of the original lamellae into small blocks.

2. Experimental

2.1. Hydrostatic extrusion

The apparatus used and details of processes of hydrostatic extrusion have been described in the

previous paper [11]. Commercial rods of high density polyethylene Hizex 5100B (Mitsui Petrochemical Co Ltd) were used as the starting material. The extrusion ratio (R_E) is defined as the ratio of the cross-sectional area before and after extrusion.

2.2. X-ray diffraction

Wide-angle X-ray diffraction patterns were taken with a flat camera. Ni-filtered Cu$K\alpha$ radiation (35 kV, 15 mA) was used. Small-angle X-ray scattering patterns were taken with a vacuum camera (Rigaku–Denki), where the specimen-to-film distance was 300 mm. Ni-filtered Cu$K\alpha$ radiation (50 kV, 90 mA) by means of Rota Unit RU-3SH (Rigaku–Denki), and pinhole collimators, 0.3 and 0.2 mm diameter, were used.

In order to estimate the crystallite size, diffraction profiles were measured with Ni-filtered Cu$K\alpha$ radiation (40 kV, 25 mA) and a scintillation counter in conjunction with a pulse-height analyser. Intensities were counted at 0.05° intervals of the Bragg angle (2θ) by means of point-count techniques.

2.3. Density

The density (ρ) was measured by the density gradient column method in a mixture of ethanol and water at 25° C. The density distribution in the column was determined by the use of calibrated glass beads.

2.4. Vickers hardness

The hardness of the extruded product was measured by a micro-hardness tester MVK (Akashi Micro Vickers Hardness Tester). A 136° diamond pyramid indenter was used. The specimen was indented under a load of 100 g and the impression measured using a microscope. For convenience, the Vickers hardness number (H_V) was calculated from the length of the diagonal parallel to the extrusion direction.

3. Results and discussion

3.1. Structural changes along the central flow line of extrudate in the die cone

3.1.1. Small- and wide-angle X-ray diffraction (SAXD and WAXD) patterns

Part 5 dealt with the small- and wide-angle X-ray diffraction (SAXD and WAXD) photographs of extruded products. This study is the direct extension of the work already reported [11]. Fig. 1 shows the X-ray diffraction patterns in the central flow line of polyethylene extruded at 80° C. Hydrostatic extrusion was stopped halfway, and the specimen was cut out of the polymer which remained in the extrusion die cone. As the deformation ratio (R), the ratio of the cross-sectional area of rod before extrusion to that of the tapered portion after deformation, was used.

As shown in Fig. 1, the SAXD and WAXD patterns from the starting material exhibit almost random crystalline orientation. With increasing deformation, the circular WAXD pattern gradually loses intensity in the meridian direction, and the SAXD pattern becomes elliptical. The WAXD pattern obtained at deformation ratio, $R = 2.87$ shows equatoral maximum on the (2 0 0) ring. The (1 1 0) diffraction has a very wide intensity distribution along the azimuthal angle. The SAXD pattern consists of four distinct intensity maxima which align so as to constitue an ellipse having the long axis on the equator. Besides these four maxima, two faint lines perpendicular to the meridian can be observed. At $R = 4.0$, the (1 1 0) and (2 0 0) diffractions are on the equator. The SAXD photograph shows a pattern with intensity maxima on the meridian, and four faint lines parallel to the equator are also observed. The WAXD photograph at $R = 6.0$ shows clearly the c-axis orientation pattern known as a "fibre diagram". The a- and b-axes are aligned perpendicular to the extrusion direction. The SAXD photograph shows a line-shaped two-point pattern. Both the WAXD and SAXD patterns for the extruded product ($R = 9.0$) show a highly oriented fibre diagram and the a- and b-axes are well aligned transversely. Aximuthal scannings of (2 0 0) and (0 2 0) reflections were carried out and the degree of c-axis orientation (f_c) was calculated using Hermans' type orientation function [14]. The degree of c-axis orientation (f_c) reached a value of 0.972 [11].

3.1.2. Crystallite size

To achieve a better understanding of the process of plastic deformation during hydrostatic extrusion of polyethylene, it is desirable to compare crystallite sizes estimated along the central flow line of the extrudate. Crystallite sizes were calculated from the wide-angle X-ray line-broadening data using the well-known Scherrer equation. The mean dimension of the crystallite normal to the planes

(0 2 0), l_{020}, is given by

$$l_{020} = k\lambda/(\beta \cos\theta), \qquad (1)$$

where λ is the wave length of radiation, β is the integral breadth of the (0 2 0) reflection expressed in radians and corrected for instrumental broadening, and cos θ is the cosine of the Bragg angle. The constant k is geometry-dependent and has been taken equal to unity. It has been assumed that lattice distortion and paracrystallinity make negligible contributions to the line broadening. The figures must, therefore, be regarded as only approximate.

Fig. 2 shows the change in l_{020} which take place during hydrostatic extrusion. The rate of reduction of crystallite size is, at first, quite fast, but with further deformation, l_{020} appears to be constant beyond $R > 4$. When the original lamellae break into small blocks, the deformation process involves intralamellar slip and rotation of the block. Closer examination of the SAXD and WAXD patterns (Fig. 1) reveals that the drastic reduction of crystallite size was accompanied by a complex change in fine structure and a considerable degree of orientation of the molecules. At a higher extrusion ratio, $R > 4$, the continuous in-

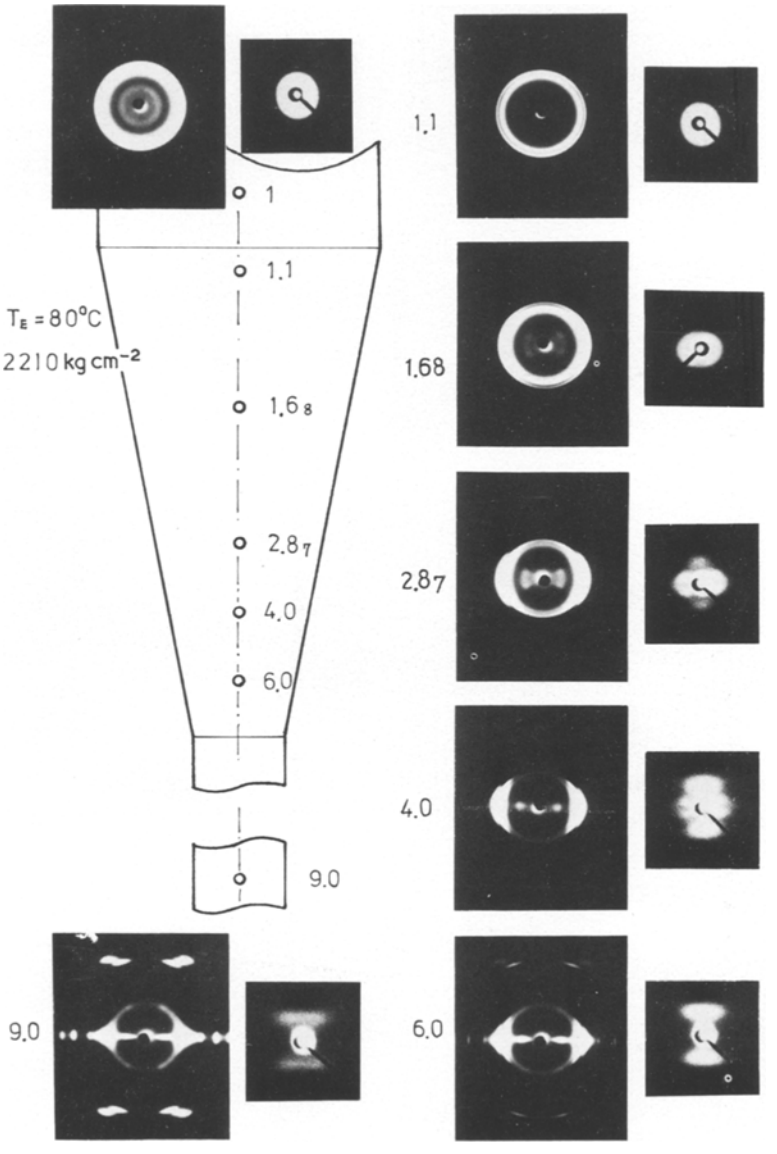

Figure 1 Small- and wide-angle X-ray diffraction (SAXD and WAXD) patterns in the central flow line of polyethylene extruded at 80° C. The specimen was cut out of the polymer which remained in the extrusion die cone.

crease of molecular orientation must be caused by the slip between the small blocks of folded-chain crystallites and by rotation of the blocks to the extrusion direction. In addition, the plastic deformation process is accompanied by rearrangement of small blocks of folded-chain crystallites and formation of highly oriented fibre structure.

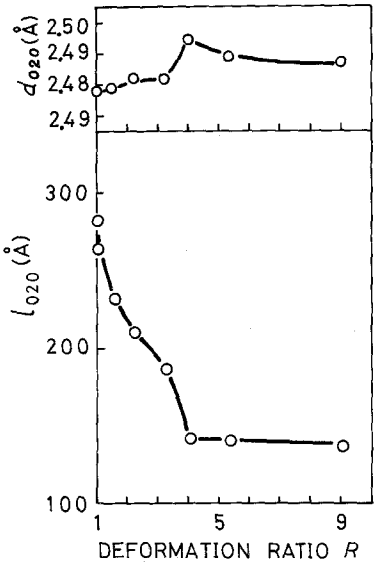

Figure 2 Change in mean dimension of crystallite normal to (0 2 0) planes, l_{020}, and spacing of (0 2 0) planes, d_{020}, along the central flow line of extrudate.

Also shown in Fig. 2 is the change in the spacing of planes (0 2 0), d_{020}, which took place during hydrostatic extrusion, Below $R < 4$, d_{020} is seen to increase with increasing deformation, or with decreasing l_{020}. Clearly, the crystallites were deformed severely, in addition to the breakdown of lamellae into small blocks.

Measurement of the density along the flow line of extrudate gives additonal information about structural changes resulting from the extrusion process. Fig. 3 shows the changes in density of polyethylene which take place during extrusion. It is seen that the density decreases progressively as the deformation ratio increases. In later stages of deformation, however, the density begins to increase. This particular property arises from the plastic deformation process of the original spherulitic structure and the formation of fibre structure.

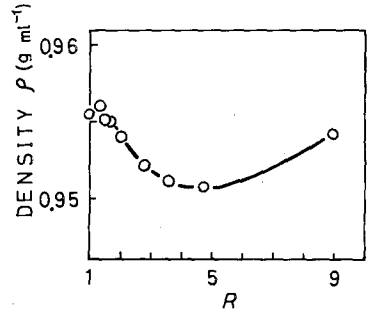

Figure 3 Change in density along the central flow line of the extrudate.

3.1.3. Long period

In the discussion of the fine structure of polyethylene, the long period determined by SAXD was used frequently to determine the changes in lamellar periodicity. Peterlin *et al.* investigated the changes in long period of the drawing process in the neck of polyethylene [15] and polpropylene [13].

The long periods calculated from SAXD patterns (Fig. 1) in the central flow line of polyethylene extruded at 80° C are plotted in Fig. 4 as a function of the deformation ratio. Schematic drawings of the SAXD patterns are shown simultaneously in Fig. 4. The equatorial long period increases slightly at first, but with increasing deformation it decreases. The circular and elliptical SAXD patterns existed only at the first stages of deformation. At the intermediate stage ($R = 2$ to 4), the SAXD patterns showed diagrams consisting of diagonal maxima and meridional maxima. The diagonal long period was nearly constant (205 to 210 Å). In further stages of deformation, the SAXD patterns showed two intensity maxima elongated perpendicular to the meridian. The meridional long period (i.e. the axial long period) decreased slightly with increasing deformation.

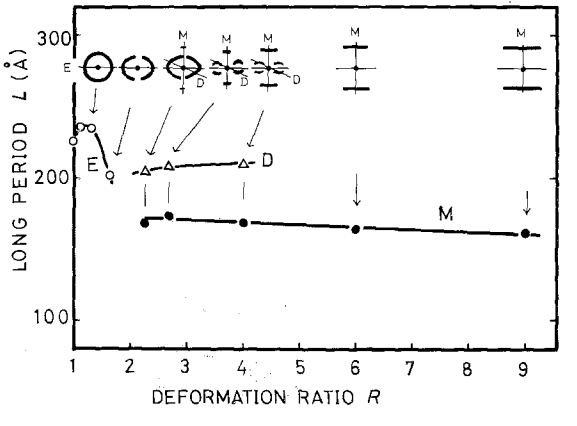

Figure 4 Long period (L) calculated from SAXD patterns (Fig. 1) and schematic drawing of SAXD patterns. M : meridional, D : diagonal, E : equatorial.

3.2. Effects of extrusion conditions on the structure and properties of extrudates

3.2.1. Crystallite size and density

The process of plastic deformation during hydrostatic extrusion of polyethylene has been already discussed to some extent. Further examination of the effects of extrusion conditions on the structure of extrudates is a matter of great technical importance. Fig. 5 shows the crystallite size l_{020} normal to planes (0 2 0). The crystallite size decreases monotonically with extrusion ratio (R_E), but with increasing extrusion ratio the rate of reduction of crystallite size slows down. The effect of extrusion temperature on the reduction of l_{020} is striking. At lower temperatures, the rate of reduction becomes relatively fast, indicating that at lower temperatures the original lamellae of polyethylene may easily undergo drastic deformation and be subdivided into small blocks.

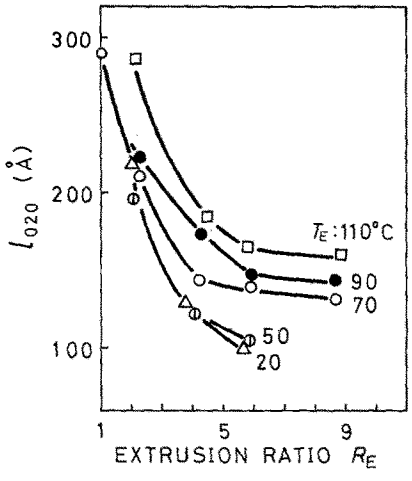

Figure 5 Crystallite size normal to (0 2 0) planes, l_{020}, versus extrusion ratio. Extrusion temperature (T_E); 20 to 110° C.

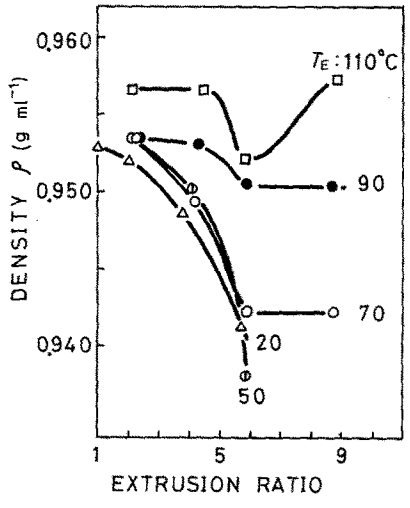

Figure 6 Density of extrudate versus extrusion ratio.

Fig. 6 shows the changes in density of extrudates at different extrusion temperatures (T_E). The density changes remarkably with extrusion ratio (R_E). At temperatures below 70° C, the density decreases drastically with extrusion ratio, whereas at higher temperatures ($T_E = 90$ to 110° C) the decrease in density with extrusion ratio is quite small. At $T_E = 110$° C, density again increases with increasing extrusion ratio, the minimum occurring at $R_E \simeq 6$. Such a sequence of changes in density with extrusion ratio is equivalent to similar changes of crystallite size.

3.2.2. Hardness

It is a well known fact that the molecular orientation affects the physical properties of a polymer. The molecular orientation is necessary for the production of fibre, film and sheet. As an example of the mechanical properties of extruded products, the hardness was measured by means of a microhardness tester.

As mechanical anisotropy arises from a combination of increased strength in the direction of extrusion and reduced strength in the transverse direction, it was necessary to measure accurately the shape of the indentation. However, a slight difficulty arose in the precise measurement of the length of the diagonal perpendicular to the extrusion direction, because the extrudate has a small diameter. So, for convenience, the Vickers hardness number (H_V) was calculated from the length of diagonal parallel to the extrusion direction.

Fig. 7 shows the relationships between the

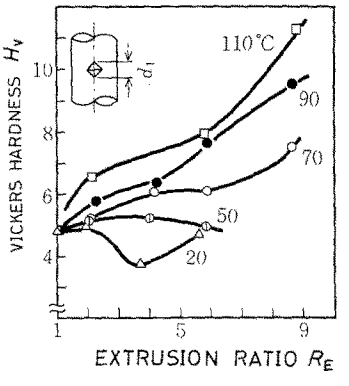

Figure 7 Relationships between the Vickers hardness number and extrusion ratio.

Vickers hardness number, H_V (kg mm^{-2}), and extrusion ratio, R_E. At low extrusion temperature ($T_E = 20^\circ$ C), H_V decreases initially, while at $T_E = 50^\circ$ C, the value remains virtually unchanged. At higher extrusion temperatures (70 to 110° C), H_V increases with increasing extrusion ratio.

It is well known that there is a close relationship between the elastic modulus and the hardness of the material. The dynamic tensile modulus for polyethylene extruded at higher temperatures increases with increasing extrusion ratio [16]. There is very little doubt that the Vickers hardness number also depends on the tensile modulus to some extent. However, in order to determine the relationship between the hardness and structure of the extrudates, it is necessary to also consider the molecular orientation, crystallinity and the fibrosity of the extrudates. A more detailed analysis of the hardness of extrudates with larger diameters will be reported in the near future.

3.2.3. Thermal contraction

When an oriented semi-crystalline polymer is heated, it will tend to shrink back towards its unoriented state. In general, the thermal shrinkage is affected by the molecular orientation and the fine-structure of specimen. The thermal contraction behaviour is of great importance in the study of an oriented polymer; it is of practical importance, being concerned directly with dimensional instability at elevated temperatures.

Table I gives the thermal shrinkage (S) of extrudates and the degree of orientation before heating. Samples were allowed to shrink whilst being annealed for 30 min at 100° C in water. The percentage thermal shrinkage was calculated from $S = 100\ (l_e - l_s)/l_e$, where l_e and l_s were lengths of the extruded sample and the annealed and shrunk sample, respectively,. Thermal shrinkage decreases with increasing extrusion ratio. It is interesting that the extrudate indicating the highest degree of crystalline and amorphous orientation exhibits thermal stability.

TABLE I Thermal shrinkage of extrudates at 100° C in water, extrusion temperature (T_E) = 70° C

Extrusion ratio R_E	Degree of orientation		Shrinkage at 100° C (%)
	Crystallite f_c	Amorhpous f_a	
2.2_3	0.519	0.03	24.5
4.1_7	0.775	0.65	12.8
5.8_8	0.938	0.69	11.3
8.6_3	0.974	0.83	4.2

Okajima *et al.* [17] studied the change in the thermal contraction and the dichroic orientation of poly(ethylene terephthalate) filament dyed with Disperse Red 17. They concluded that the thermal contraction was caused principally by the disorientation of amorphous chains. This conclusion was supported by the results of the study of dichroism at high temperatures [18].

In the case of hydrostatically extruded polyethylene, the higher the degree of orientation of amorphous chains, the greater would be the expected shrinkage. However, the extrudate with a higher degree of amorphous orientation shrank little (Table I), indicating that the extrudate has a highly oriented fibre structure which is closely filled with fully oriented crystallites. In Part 5 [11], the outstanding properties of our products, i.e. transparency and fibrosity, could be accounted for by a typical fibre structure. The extrudate having a high extrusion ratio consists of stacks of highly oriented crystallites and interfibrillar amorphous bundles. It is easy to consider that the stack of highly oriented crystallites would restrict the thermal contraction of the interfibrillar amorphous chain bundles.

4. Conclusions

As a direct extension of work already reported [11], the structural changes along the central flow line of an extrudate were investigated in detail. The effects of extrusion temperature and extrusion ratio on the plastic deformation of polyethylene were also studied. The results and conclusions can be summarized as follows:

(1) The X-ray diffraction patterns along the central flow line of the extrudate were useful in understanding the process of plastic deformation of polyethylene during hydrostatic extrusion.

(2) Drastic reduction in crystallite size at low deformation ratios was accompanied by a complex change in fine structure. In addition, a considerable degree of orientation and severe deformation of the crystallite itself took place.

(3) At higher deformation ratios, $R > 4$, the continuous increase in molecular orientation was caused by the rotation of small blocks of crystallite to the extrusion direction.

(4) At higher extrusion temperatures ($T_E = 70$ to 110° C), the Vickers hardness number of extruded polyethylene increased with increasing

extrusion ratio.

(5) The extrudate with the highest extrusion ratio shrank little when annealed at 100° C in water.

References

1. I. L. HAY and A. KELLER, *J. Mater. Sci.* **1** (1966) 41.
2. T. SETO, T. HARA and K. TANAKA, *Jap. J. Appl. Phys.* 7 (1968) 31.
3. R. CORNELIUSEN and A. PETERLIN, *Makromol. Chem.* **105** (1967) 193.
4. K. IMADA, T. YAMAMOTO, K. SHIGEMATSU and M. TAKAYANAGHI, *J. Mater. Sci.* **6** (1971) 537.
5. R. S. STEIN and F. H. NORRIS, *J. Polymer Sci.* **21** (1956) 381.
6. G. MEINEL, N. MOROSOFF and A. PETERLIN, *J. Polymer Sci. A2* 8 (1970) 1723.
7. K. NAKAYAMA and H. KANETSUNA, *Kobunshi Kagaku* **30** (1973) 713.
8. *Idem, Kobunshi Ronbunshu* **31** (1974) 256.
9. *Idem, ibid* **31** (1974) 321.
10. K. NAKAYAMA, K. SATAKE, T. OKI and H. KANETSUNA, *J. Jap. Soc. Tech. Plasticity* **15** (1974) 744.
11. K. NAKAYAMA and H. KANETSUNA, *J. Mater. Sci.* **10** (1975) 1105.
12. N. KASAI and M. KAKUDO, *J. Polymer Sci. A* 2 (1964) 1955.
13. F. J. BALTÁ-CALLEJA and A. PETERLIN, *J. Macromol. Sci. B* 4 (1970) 519.
14. P. H. HERMANS, "Physics and Chemistry of Cellulose Fibres" (Elsevier, Amsterdam, 1949).
15. A. PETERLIN and G. MEINEL, *Makromol. Chem.* **142** (1971) 227.
16. K. NAKAYAMA, unpublished data.
17. S. OKAJIMA and K. YAO, *Sen-i Gakkaishi* **22** (1966) 17.
18. K. NAKAYAMA, S. OKAJIMA and Y. KOBAYASHI, *J. Appl. Polymer Sci.* **13** (1969) 659.

Received 25 August and accepted 22 October 1976.